



Preparation of bactericidal surfaces with high quaternary ammonium content through photo-initiated polymerization of N-[2-(acryloyloxy)ethyl]-N,N-dimethyl-N-butylammonium iodide from native and thiolated PDMS surfaces

Yuzhen Lou, Damien Schapman, Dimitri Mercier, Stephane Alexandre, Fabrice Burel, Pascal Thebault, Nasreddine Kébir

► To cite this version:

Yuzhen Lou, Damien Schapman, Dimitri Mercier, Stephane Alexandre, Fabrice Burel, et al.. Preparation of bactericidal surfaces with high quaternary ammonium content through photo-initiated polymerization of N-[2-(acryloyloxy)ethyl]-N,N-dimethyl-N-butylammonium iodide from native and thiolated PDMS surfaces. *Reactive and Functional Polymers*, 2021, 165, pp.104941. <10.1016/j.reactfunctpolym.2021.104941>. <hal-03357259>

HAL Id: hal-03357259

<https://hal.science/hal-03357259v1>

Submitted on 30 Sep 2021

HAL is a multi-disciplinary open access archive for the deposit and dissemination of scientific research documents, whether they are published or not. The documents may come from teaching and research institutions in France or abroad, or from public or private research centers.

L'archive ouverte pluridisciplinaire **HAL**, est destinée au dépôt et à la diffusion de documents scientifiques de niveau recherche, publiés ou non, émanant des établissements d'enseignement et de recherche français ou étrangers, des laboratoires publics ou privés.



HAL Authorization

Preparation of bactericidal surfaces with high quaternary ammonium content through photo-initiated polymerization of *N*-[2-(acryloyloxy)ethyl]-*N,N*-dimethyl-*N*-butylammonium iodide from native and thiolated PDMS surfaces

Yuzhen Lou¹, Damien Schapman², Dimitri Mercier³, Stephane Alexandre⁴, Fabrice Burel¹, Pascal Thebault⁴, Nasreddine Kébir¹

¹ Normandie Université, INSA Rouen Normandie, Laboratoire PBS, UMR CNRS 6270 & FR 3038, Avenue de l'Université, 76801 Saint Etienne du Rouvray, France

² Normandie Université, UNIROUEN, IFR MP 23, PRIMACEN, 76821 Mont-Saint-Aignan, France

³ PSL Research University, Chimie ParisTech – CNRS, Institut de Recherche de Chimie Paris, 11 rue Pierre et Marie Curie, 75005 Paris, France

⁴ Normandie Université, UNIROUEN, laboratoire PBS, UMR CNRS 6270 & FR 3038, 76821 Mont-Saint-Aignan, France

Abstract

N-[2-(acryloyloxy)ethyl]-*N,N*-dimethyl-*N*-butylammonium iodide was successfully photo-polymerized from native and thiolated PDMS surface, in the presence of benzophenone. The directly and indirectly grafted surfaces exhibited quaternary ammonium densities of about 10^{15} and 10^{17} charge/cm², respectively, and very high hydrophilicity compared to non-grafted surfaces. The live and dead tests performed by fluorescence microscopy revealed an effective contact bactericidal effect of this surface against *Escherichia coli* and *Staphylococcus epidermidis*.

Keywords: Quaternary ammonium; photo; grafting from; PDMS; bactericidal; thiol

Corresponding authors: nasreddine.kebir@insa-rouen.fr; pascal.thebault@univ-rouen.fr

Introduction

Silicones, especially PDMS, is a very important family of polymer materials combining flexibility, hydrophobicity, chemical and thermal stability as well as biocompatibility. Silicone materials are widely used in the medical field, such as joint implants, catheters, kidney dialysis machines and breast prostheses [1-7]. However, like any organic material, it is subject to biofouling and bacterial contamination phenomena leading to serious health and economic problems [8]. Consequently, many approaches have been developed to overcome this problem [9-21].

The chemical tethering of antibacterial polymers onto the PDMS surface is one of the most serious routes to avoid its contamination and/or biofouling. Due to its chemical stability, PDMS often undergoes physical pretreatment, such as plasma, to generate functional anchoring sites, as for example hydroxyl groups, leading to very hydrophilic surfaces [11]. However, due to the fast diffusion of these groups within the bulk regenerating hydrophobicity, the post-chemical grafting must be performed rapidly (i.e., few minutes after) [12].

During the two last decades, two direct chemical routes for PDMS surface derivatization were described in the literature [13-21]. Hydrosilylation coupling reaction was used to graft bioactive polymers or molecules bearing carbon-carbon double bonds onto PDMS surface presenting Si-H groups [13-18]. The extent of Si-H groups can be varied by tuning the ratio between the PDMS components and/or their curing time [13-16]. Si-H groups can also be inserted on the surface by an acid-catalyzed reaction with poly(methylhydroxysiloxane) [17-18]. The use of the hydrosilylation process to prepare bactericidal PDMS surface bearing quaternary ammonium (QA) groups has been described in the work of Kebir *et al.* [13]. The authors synthesized a Poly(*N,N*-dimethylbutyl vinylbenzyl ammonium chloride) copolymer bearing carbon-carbon double bonds and grafted it by hydrosilylation onto PDMS surfaces. The extent of polymer grafting was tuned by varying the Si-H content through variations performed on the curing time or the relative composition in the silicone components. The charge densities of the obtained cationic PDMS surfaces ranged from 1.8×10^{14} to $2.8 \times 10^{15} \text{ N}^+ \cdot \text{cm}^{-2}$ and the contact angle with water (WCA) varied from 102 and 88°, respectively. However, the direct grafting on fully cured PDMS offered the lowest surface coverage and wettability. Nevertheless, high killing efficiency (96-100%, respectively) against *E. coli* and *S. epidermidis* after 1h of contact was obtained in all cases.

Photo-induced grafting, in presence of benzophenone, have also been used in few studies for the direct chemical modification of PDMS surfaces. Thus, acrylic acid, [19] polyethylene

glycol monoacrylate and polyethylene glycol diacrylate [20] have been photo-grafted through a mask to prepare micropatterned PDMS surfaces. Recently, antifouling PDMS surfaces were designed through simultaneous photo-grafting/photo-crosslinking reactions of zwitterionic polymers, i.e. poly(sulfobetaine methacrylate) or poly(carboxybetaine methacrylate), using poly(ethylene) glycol diacrylate as crosslinker [21].

Thus, in this work, we describe the use of this straightforward photochemical process to prepare highly QA-functionalized bactericidal cationic PDMS surfaces through surface photo-initiated radical polymerization of *N*-[2-(acryloyloxy)ethyl]-*N,N*-dimethyl-*N*-butylammonium iodide, in the presence of benzophenone as photo-initiator. The main objective of this work is to prepare new QA-PDMS surfaces with high bactericidal longevity and hydrophilicity comparing to analogues prepared by the hydrosilylation process. In addition, cationic PDMS surface with grafted acrylate ammonium chains have never been prepared neither by the hydrosilylation ‘grafting to’ nor by the photochemical ‘grafting from’ processes. It is to note that each chemical structure of the grafted polymer brings to the surface original physico-chemical properties and biological activity spectra. We will start by describing the optimization of this process on the native and fully cured PDMS surface. Then, in order to increase the reactivity of this surface, thiol groups will be introduced (PDMS-T), using the same photochemical process. The polymer grafting on the native and thiolated PDMS surfaces will be studied by FTIR-ATR and XPS spectroscopies as well as by contact angle and charge density measurements. The antimicrobial properties of the cationic surfaces will be investigated by the live and dead fluorescent test.

Experimental section

Materials

Sylgard[®] 184 was purchased from DOW chemical company (USA). 2-(dimethylamino)ethyl acrylate (98%) (DMAEA) and 1-iodobutane (99%) were purchased from Alfa Aesar. Dry methanol (99,8%), acetone and extra dry acetonitrile were purchased from Acros Organics. Pure hydroquinone was purchased from Prolabo. Dry diethyl ether and glass coverslip (18 mm×18 mm, Fisherbrand[™]) were purchased from Thermo Fisher Scientific. Pentaerythritol tetrakis (3-mercaptopropionate) (PTTMP) was purchased from Aldrich. Benzophenone (BP) (≥99%) was purchased from Merck. Ultrapure water was obtained from a Milli-Q system (Siemens, France). All the chemicals were used without further purification.

S. epidermidis (ATCC 35984) and *E. coli* (K12 MG1655) strains were stored as frozen aliquots in brain heart infusion (BHI, Bacto, France) broth and 30 % of glycerol at -20 °C. The LIVE/DEAD Bacterial Viability Kit, L7007 (SYTO[®]9 dye, 1.67 mM / Propidium iodide, 18.3 mM) was purchased from Thermo Fisher Scientific. All solutions used for the antibacterial assay were sterilized by autoclave (121°C, 15 min).

Preparation of *N*-[2-(acryloyloxy)ethyl]-*N,N*-dimethyl-*N*-butylammonium iodide (AONAI)

N-[2-(acryloyloxy)ethyl]-*N,N*-dimethyl-*N*-butylammonium iodide (AONAI) was synthesized according to a procedure described in the literature, [22-24] with some modifications. Briefly, in a three-neck round-bottom flask equipped with magnetic stirring and a condenser, 1-iodobutane (0.0703 mol) and 2-(dimethylamino)ethyl acrylate (DMAEA) (0.06586 mol) were added dropwise to a vigorously stirred solution of dry acetonitrile (30 ml) containing a small amount of hydroquinone (0.03 g) at 40 °C under inert atmosphere. The mixture was left to react 48h under stirring. Then, the mixture was concentrated and added dropwise into a large excess (10 folds in volume) of dry diethyl ether. After 30 min, the recrystallized product was collected by filtration and dried under vacuum.

¹H NMR (300 MHz, DMSO) δ : 6.39 (dd, $J = 17.3$ and 1.7 Hz, 1H), 6.21 (dd, $J = 17.1$ and 10.3 Hz, 1H), 6.05 (dd, $J = 13.7$ and 1.5 Hz, 1H), 4.55 (s, 2H), 3.79 – 3.61 (m, 2H), 3.41 – 3.35 (m, 2H), 3.11 (s, 6H), 1.81 – 1.56 (m, 2H), 1.37 – 1.15 (m, 2H), 0.94 (t, $J = 7.5$ Hz, 3H). FTIR-ATR (cm⁻¹): 3031 (=C-H stretching vibration); 3000-2800 (C-H stretching vibration in CH, CH₂ and CH₃ groups); 1730 (C=O stretching vibration of the ester group); 1634(C=C stretching vibration of the vinyl group); 1491 (C-H bending vibration in N⁺-CH₂ (ester side)); 1464 (C-H bending vibration in N⁺-CH₂ (butyl chain side)); 1448 (C-H bending vibration in N⁺-CH₃); 1406 (=C-H bending vibration); 1063 (C-N stretching vibration).

Preparation of PDMS film

15 g of a mixture of the two parts of Sylgard[®] 184, i.e. base and curing agent, at a ratio of 10:1 (w/w), were casted into a low-density polyethylene petri dish square (120×120×17 mm³). The mixture was then degassed under vacuum, until the air bubbles were completely removed. The PDMS film was formed after two days at room temperature and was cut into 18 × 18 mm² squares with a thickness less than 1 mm. The curing time can be considerably reduced by increasing the temperature (few hours at 70°C and about 1h at 120°C) [13].

Preparation of PDMS-PAONAI and PDMS-TPAONAI surfaces

PDMS films were first immersed in an acetone solution containing 20 wt% of BP for 30 min to absorb enough BP for the photo-grafting. The samples were quickly washed with methanol and then placed on a plate to dry in the dark. Then 50 to 80 μ l of an acetone solution containing PTTMP was applied to the dry samples and covered with a glass slide so that the PTTMP solution was spread evenly over the surface of the PDMS by capillary force. The PDMS assembly was placed in a UV conveyor (UV Fusion Light Hammer 6), and irradiated with the UV light emitted from a small diameter electrodeless bulb combined with the elliptical reflector, microwave-powered lamp (500 watts/inch) at a lamp-PDMS distance of 53 mm. Then, the BP-initiated photo grafting and photopolymerization of the PTTMP took place from the PDMS surface. After grafting, substrates were collected and washed in acetone overnight with slight shaking and washed again with acetone the next day before drying to remove all unreacted BP or PTTMP. The substrates were noted PDMS-T. Then, photopolymerization were realized by using the methanol solution containing AONAI in the same way on substrate of PDMS or PDMS-T and they were noted PDMS-PAONAI and PDMS-TPAONAI, respectively.

After modification, the samples were collected by immersion in water to detach from the glass slide and then washed with methanol three times. Then, the samples were washed in methanol overnight with slight shaking and washed again with methanol the next day before vacuum drying to ensure that all unreacted monomer and ungrafted BP or AONAI compounds were removed.

Characterizations

^1H NMR spectra were recorded on a Bruker 300 MHz spectrometer. The ATR-FTIR spectra were recorded on a Nicolet IS-50 FTIR (Thermo, USA) spectrometer using the VariGATR accessory (Harrick Scientific, Pleasantville, NY) and the DTGS detector on three independent samples for each experimental condition, with a wave-number range between 600 and 4000 cm^{-1} . The data was obtained with a spectral resolution of 4 cm^{-1} by 250 scans.

Static and dynamic water contact angles measurements were performed using a contact angle goniometer “digidrop” (United Kingdom) in air at room temperature on at least three independent samples.

X-Ray Photoelectron spectroscopy (XPS) analysis was performed using a Thermo Electron Escalab 250 spectrometer, with a monochromatic Al K α X-ray source ($h\nu = 1486.6\text{eV}$) operating at a pressure around 10^{-9} mbar. The spectrometer was calibrated using Au4f7/2 at 84.1eV. The take-off angle was 90° and the analyzed surface was a 500 μm diameter disk. Survey spectra were recorded with a pass energy of 100eV and a step of 1eV and C1s, O1s, Si2p high level resolution spectra were recorded with a pass energy of 20eV and a step of 0.1eV. The charge effect was evaluated using the main component of the C1s peak, associated with C-C/C-H hydrocarbons with a binding energy of 285eV. Spectra were recorded using the Thermo Advantage software and analyzed using CasaXPS software.

The topography of PDMS surfaces before and after modification were analyzed by using a Nanoscope 8 Multimode microscope (Bruker Nano Surfaces, Santa Barbara, CA, USA). Imaging was achieved in the air using the PeakForce®-QNM mode with a 100 μm piezoelectric scanner. A silicon (RTESPA-300, Bruker) cantilever with a spring constant of about 40 N/m and a silicon tip was used. Images were obtained with a PeakForce tapping frequency of 1 kHz and the auto-amplitude on. The AFM imaging was performed in multiple locations on at least two independent samples at two scan sizes: 5 x 5 and 20x20 μm^2 . All images are presented in the height mode and are top view images. Flatten & three points levelling operations were usually done using the Gwyddion AFM software.

Determination of the surface accessible quaternary ammonium density

Modified and unmodified PDMS surfaces ($1.8 \times 1.8\text{ cm}^2$) were immersed in a solution of fluorescein sodium salt (1% in distilled water) for 10 min. Afterwards, the unreacted fluorescein molecules were removed by washing with distilled water. The samples were then placed in 3 mL of a 0.5% solution of hexadecyltrimethyl ammonium bromide to exchange with the bounded fluorescein molecules under ultrasound for 15min. 0.45 mL of saturated NaHCO_3 solution was added after sonication. Then the absorbance of solution was recorded at 501 nm. The fluorescein concentration was then calculated using a calibration curve.

Antibacterial activity assay (Live/Dead test)

A 130 μl droplet of *E. coli* or *S. epidermidis* suspension in distilled water (5.8×10^8 cells/ml) was spread on the modified surfaces ($1.8\text{ cm} \times 1.8\text{ cm}$) using a glass slide with the same surface size for 1 h. Then the glass slide was taken away and the studied surface was washed by distilled water flow to remove the non-attached bacteria. After that, a 130 μl mixture of two

fluorescent markers: the SYTO[®] and the propidium iodide, was deposited and spread on the surface for 15 min. The mixture was diluted prior to use (20 µmol/l of SYTO[®]9). Images (1024x1024 pixels) of surfaces were acquired using an upright fixed-stage Leica TCS SP8 CFS confocal microscope (Leica Microsystems, Nanterre, France) equipped with diodes laser (Coherent, Les Ulis, France) at 488 nm to excite the SYTO[®]9 and at 552 nm to excite Propidium Iodide and a conventional scanner at 400 Hz. Using a 63x (1.40, oil immersion) objective, fluorescence emission was sequentially detected through hybrid detector (Leica Microsystems, Nanterre, France) in photon counting mode with a specific band from 500 to 540 nm for SYTO[®]9 and 580 to 630 nm for Propidium Iodide. Z-Stack's images were acquired using an adapted step-size from Nyquist Criteria. ImageJ (Rasband W.S., U.S. National Institutes of Health, Bethesda, Maryland, USA, <http://imagej.nih.gov/ij/>, 1997-2020) was used to adjust brightness and contrast and to perform z projections of 3D images (xyz) [25].

Results and discussion

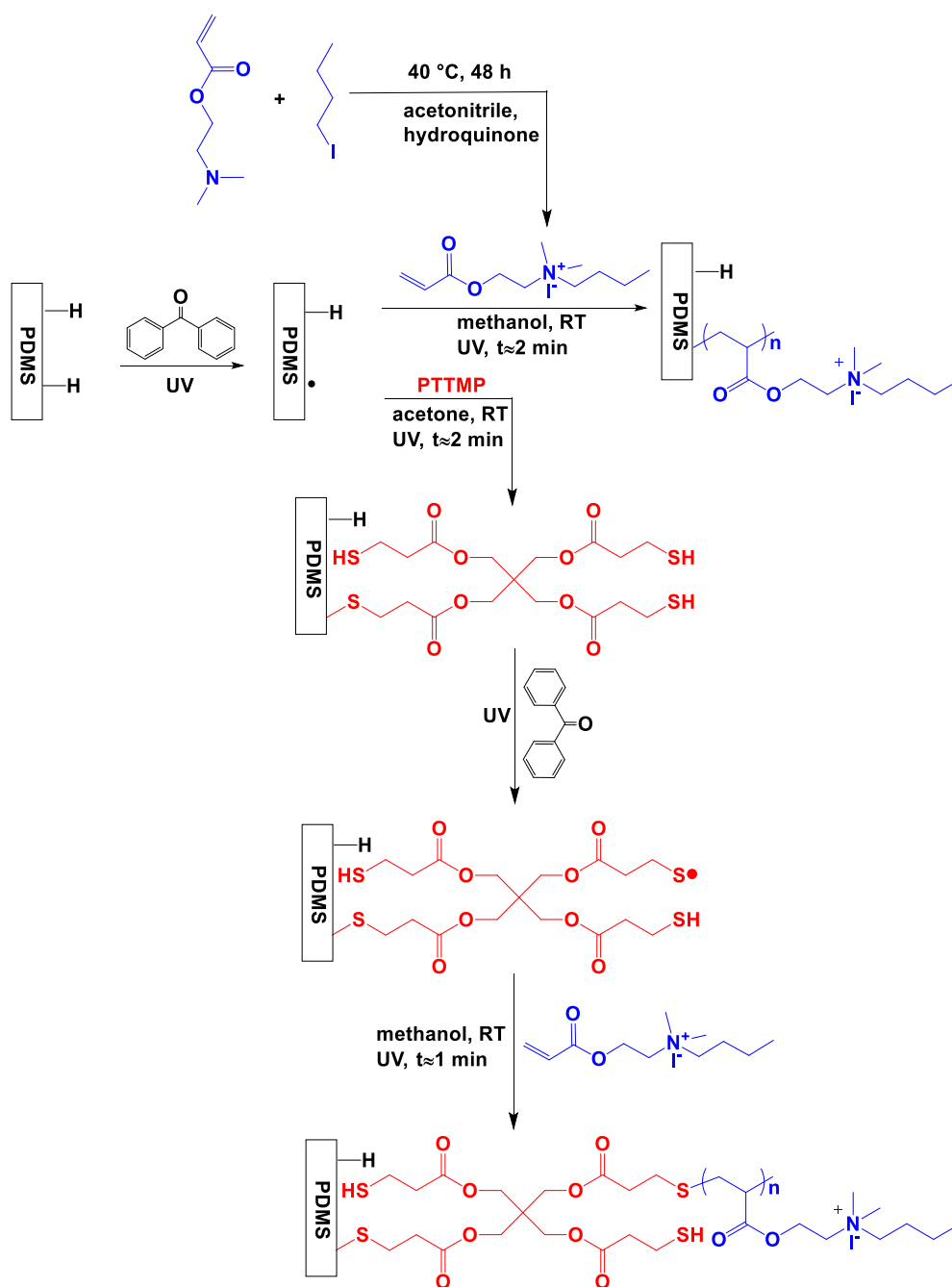
Cationic polymers bearing quaternary ammonium (QA) groups exhibit high biocidal activity against bacteria, fungi, parasites and viruses. Moreover, this activity is dramatically dependent on the chemical structure of the polymer involving the hydrophilic-hydrophobic balance, the molecular weight and the length or nature of the alkyl chains of the QA groups [26-34]. For instance, Lu *et al.* [33] have prepared by quaternization poly(dimethylaminoethyl methacrylate (poly(DMAEMA)) with benzyl chloride (BC), butyl bromide (BB), dodecyl bromide (DB) or hexadecyl bromide (HB) and have found that polymers quaternarized with BC and BB exhibited the highest bactericidal activity in solution. Lafarge *et al.* [34] have prepared a copolymer based on poly(DMAEMA), quaternarized with butyl iodide and bearing propargyl groups, and have grafted it onto azidated PVC surface by the click HDC cycloaddition. The obtained cationic PVC surfaces exhibited a high bactericidal effect against *E. coli* and *S. epidermidis*.

In this work, we study the photo-initiated surface radical polymerization of *N*-[2-(acryloyloxy)ethyl]-*N,N*-dimethyl-*N*-butylammonium iodide (AONAI) from native and thiolated PDMS surfaces, in order to design high QA-functionalized bactericidal surface. We anticipated that this process will offer a grafted polymer with an appropriate molecular weight and/or surface charge density that promotes high and long-term bactericidal effect on the PDMS surface.

Study of the direct photo-initiated polymerization of AONAI from native and thiolated PDMS surfaces (preparation of PDMS-PAONAI and PDMS-T-PAONAI)

N-[2-(acryloyloxy)ethyl]-*N,N*-dimethyl-*N*-butylammonium iodide (AONAI) monomer was synthesized by the reaction of 1-Iodobutane with 2-(dimethylamino)ethyl acrylate (DMAEA) in acetonitrile at 40°C for 48h, in the presence of hydroquinone as a stabilizer avoiding the self-polymerization of the acrylate monomer. The pure monomer was obtained by recrystallization and was soluble in water and alcohol solvents.

The ¹H NMR spectrum of the obtained monomer mainly revealed the signals of protons of the carbon-carbon double bonds at 6.02 to 6.38 ppm and the protons of methyl and methylene groups in the α position to the ammonium group from 3.1 to 3.7 ppm, respectively. In addition, the FTIR analysis showed the complete conversion of the amine group into an ammonium group, through mainly the appearance of new bands at around 1491 and 900-950 cm⁻¹.



Scheme 1. Synthesis of N-[2-(acryloyloxy)ethyl]-N,N-dimethyl-N-butylammonium iodide (AONAI) and its photo-polymerization from the PDMS surface with or without Pentaerythritol tetrakis (3-mercaptopropionate) (PTTMP) pretreatment.

The radical photo-polymerization of the acrylate ammonium monomer from the native PDMS surface was initiated by benzophenone (Scheme 1) and was monitored at several reaction times (number of passages under UV) and concentrations of the started monomer solution. The studied PDMS film was a totally cured Sylgard[®]184 prepared at the conventional ratio of PartA/PartB = 1/10. A drop of the acrylate ammonium monomer solution was spread on the PDMS surface by depositing a thin glass plate on it. The sample was then placed in the UV conveyor for 1.55 s of UV exposure by passage. 50 to 90 passages were used, depending

on the grafting efficiency. Three PDMS surface controls were also prepared, i.e. untreated PDMS (control 1), PDMS treated with methanol and UV (80 passages) (control 2) and PDMS treated with a monomer solution (76wt%) during 80 passages in the conveyer without UV exposure (control 3).

The extent of polymer grafting onto silicone surfaces was evaluated by water contact angle measurements (Figures 1, Tables 1). PDMS controls (1, 2 and 3, Table 1) displayed water contact angle values around 108 ± 2 , 99 ± 7 and $105\pm 3^\circ$, respectively, which are consistent with the high hydrophobicity of PDMS and suggesting no modification of the PDMS surface properties without UV.

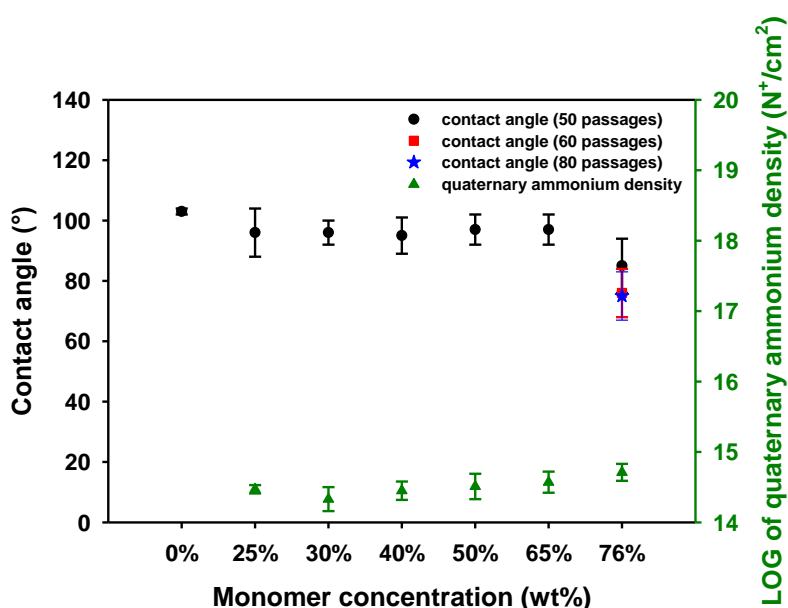


Figure 1. Water static contact angle of directly modified PDMS with a series of monomer concentration solution: 25wt%, 30wt%, 40wt%, 50wt%, 65wt% and 76%, using 50, 60 and 80 passages under UV. Values of Log of quaternary ammonium density were recorded for 50 passages.

The influence of the monomer concentration on the extent of polymer grafting onto the surface after 50 to 80 passages under UV was first studied (Figure 1). One can observe that for a monomer concentration ranging from 25 to 65 wt% and a number of passages under UV of 50, the water contact angle slightly decreased from 108° to around 95° , which suggests a weak surface grafting efficiency. For a monomer concentration at 76 wt%, the average water contact angle value decreased to around 85° . At this concentration, when the number of passages was increased to 60 or 80, the average water contact angle fell to a steady value around 75° , which was considered as the optimal value.

Measurement of the dynamic water contact angles were achieved on the optimal surface (Table 1). It is noteworthy that the advancing angle (AA) is correlated to the wettability of the

hydrophobic part of the surface while the receding angle (RA) arise from the hydrophilic part. For the direct surface modification, the values of AA, RA and the hysteresis (AA-RA) changed dramatically after the polymer grafting. The PDMS surface treated only with methanol (control 2) or with AONAI without UV (control 3) did not exhibit any significant change on the surface comparing to the native one (control 1). AA dropped from 116 to 83°, RA dropped from 58 to 9° and hysteresis increased from 57° to 74° (Table 1, control 1 and PDMS-AONAI, respectively). However, the increase of the hysteresis is usually ascribed either to a physical (roughness) and/or chemical (gradient of grafting density) heterogeneities of the prepared surface.

Table 1. Data of contact angles measurements and surface charge densities on the optimal treated PDMS surfaces and their controls.

Samples	Static θ_{water} (°) ^a	Dynamic θ_{water} (°) ^a			QA density (N ⁺ .cm ⁻²)	Roughness by AFM ^b (nm)	
		AA	RA	Hyst		Ra	RMS
PDMS (control 1)	108±2	116±3	58±4	57±2	ND	1.4	2.4
PDMS-MeOH (control 2)	99±7	121±8	45±10	77±2	ND	/	/
PDMS-AONAI without UV (control 3)	106±3	116±1	40±4	76±5	ND	/	/
PDMS-PAONAI	75±8	83±2	9±1	74±1	$(2.5\pm0.6) \times 10^{15}$	11.2	18.2
PDMS-T (control 4)	97±8	121±2	68±1	53±2	ND	2.8	3.8
PDMS-T-AONAI without UV (control 5)	103±3	116±1	39±5	77±5	ND	/	/
PDMS-T-PAONAI	28±8	44±4	15±4	29±0	$(9.6\pm0.3) \times 10^{16}$	7.6	10.2

^a θ_{water} : contact angle with water; **AA**: Advancing Angle; **RA**: Receding Angle; **Hyst**: Hysteresis (AA-RA).

^b Ra: arithmetic roughness, RMS: Mean Square roughness.

The contact killing capacity of quaternary ammonium surfaces is directly linked to their surface charge density. Indeed, it has been shown in many studies that the surface must display a minimal charge density value of 10^{14} N⁺.cm⁻² to kill effectively *E. coli* and *S. epidermidis* [13,34-37]. The charge density values of the cationic PDMS surfaces prepared at different monomer concentrations and passages are presented in Figure 1 and Table 1. One can observe

charge density values ranging from around 10^{14} to $10^{15} \text{ N}^+.\text{cm}^{-2}$. The optimal surface, obtained with a monomer solution at 76 wt% and 60 passages under UV, exhibited a charge density value of $(2.5 \pm 0.6) \times 10^{15} \text{ N}^+.\text{cm}^{-2}$ suggesting, anyway, a high potential of bacterial killing.

Overall, The direct photo-grafting process provided an effective surface modification after full crosslinking of the PDMS compared to the hydrosilylation process performed on similar surfaces [13], with respectively, charge density values around $10^{15} \text{ N}^+/\text{cm}^2$ vs. $10^{14} \text{ N}^+/\text{cm}^2$ and WCA of 76° vs. 102° . However, these values were very close to those obtained after the enhancement of the surface grafting by hydrosilylation, using partially cured PDMS or by changing the A/B ration of the Sylgard 184 components.

Thus, the direct photo-initiated polymerization of the acrylate ammonium monomer from the native PDMS surface was not sufficient to get highly functionalized quaternary ammonium surfaces, as expected for a grafting from process.

As mentioned before, to enhance quaternary ammonium density, a thiolation pretreatment of the PDMS surface was performed. Indeed, by radical-initiation process, forming radical polymerization sites from thiol groups is clearly easier than from methyl groups. Thus, a drop of pentaerythritol tetrakis (3-mercaptopropionate) (PTTMP) in methanol solution was spread on the PDMS surface by mean of a glass plate. The PTTMP concentration was varied from 25 to 75 wt% with a number of passages under UV of 50 and the number of passages was varied from 30 to 100 for a PTTMP concentration at 50 wt% (Figure 2). One can observe that, regardless the thiolation conditions, the obtained water contact angle was around 100° (against 108° for the native PDMS) suggesting a degree of modification of the PDMS surface with PTTMP. However, since PTTMP is hydrophobic, the impact of the PDMS surface modification on its wettability was not significant.

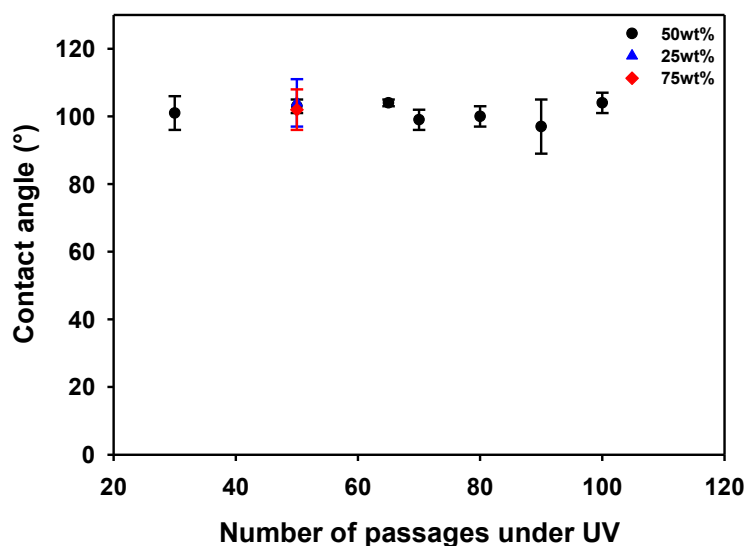


Figure 2. Water static contact angle of modified PDMS with PTTMP solution at different concentration and under several number of passages under UV.

The photo-initiated polymerization of AONAI from the thiolated surface was performed by varying the monomer concentration from 25 to 76 wt% and the number of passages from 50 to 60 with also different conditions of the thiolation step (Table 2). A monomer concentration of 76 wt% and 50 passages under UV were found to be the optimal conditions leading to the most hydrophilic and functionalized surface, with a contact angle with water around 28°. Indeed, because of solubility and viscosity concerns, the concentration cannot be increased above 76wt%. In addition, when we increased the number of passages under UV both for thiolation and photopolymerization the value of the contact angle with water remained around 28° (Table 2).

The thiolated PDMS surface (Table 1, control 4) revealed AA, RA and hysteresis values of 121, 68 and 53°, respectively. After treatment with the monomer solution in the absence of UV (control 5), a slight decrease of the RA was observed under room conditions suggesting a low degree of grafting, which attest the high reactivity of thiol groups. After the polymer grafting under UV, the optimal modified surface showed a dramatical decrease of these three parameters to 44, 15 and 29°, respectively, suggesting a very high surface coverage.

The intermediate cationic surfaces exhibited charge density values slightly above $10^{15} \text{N}^+.\text{cm}^{-2}$, whereas the optimal surface displayed a value close to $10^{17} \text{N}^+.\text{cm}^{-2}$ suggesting a very high potential of bacterial killing. These results demonstrated the importance of the pretreatment by thiolation to have the highest surface coverage and grafting density.

Thus, the optimal grafted surface exhibited higher charge density and hydrophilicity values comparing to the best QA-PDMS surface prepared by hydrosilylation. i.e $10^{17} \text{ N}^+/\text{cm}^2$, vs $10^{15} \text{ N}^+/\text{cm}^2$ and WCA of 28° vs. 88° .

Table 2. Water static contact angle and surface charge densities of modified PDMS with monomer solution by using PDMS pretreated with PTTMP (PDMS-T) under different conditions.

P(T)^a	P(AONAI)^b	C_(AONAI) (wt%)^c	θ_{water} ($^\circ$)^d	QA density ($\text{N}^+.\text{cm}^{-2}$)
50	50	25	57±26	$(4.3\pm0.7) \times 10^{15}$
50	50	30	54±25	$(3.4\pm0.6) \times 10^{15}$
50	50	40	63±24	$(3.6\pm0.04) \times 10^{15}$
50	50	50	50±28	$(1.9\pm0.1) \times 10^{15}$
50	50	65	52±20	$(1.8\pm0.5) \times 10^{15}$
70	50	65	56±21	/
80	50	65	51±21	/
90	50	65	45±20	/
90	50	76	28±8	$(9.6\pm0.3) \times 10^{16}$
100	60	76	27±11	/

^a Number of passages under UV of PDMS with 50wt% PTTMP solution.

^b Number of passages under UV of PDMS-T with monomer solution.

^c The concentration of monomer.

^d θ_{water} : contact angle with water.

In summary, for all the next studies, the direct modification of the native PDMS surfaces was performed with a monomer solution at 76 wt% with 60 passages under UV and the indirect modification was performed on thiolated PDMS surfaces treated with a monomer solution at 76 wt% with 50 passages under UV (Table 1). For the thiolation step, a solution of PTTMP at 50 wt% with 90 passages under UV was used (Table 2).

Surface characterization by AFM

AFM analyses revealed the structural and topographical changes on the PDMS surfaces after thiolation as well as after direct and indirect photo-chemical polymerizations of the cationic monomer (Figure 3). The roughness values of the prepared PDMS surfaces compared to their controls are presented in Table 2. The native PDMS exhibited a very smooth surface with an arithmetic roughness of around 1.4 nm (Figure 3-A).

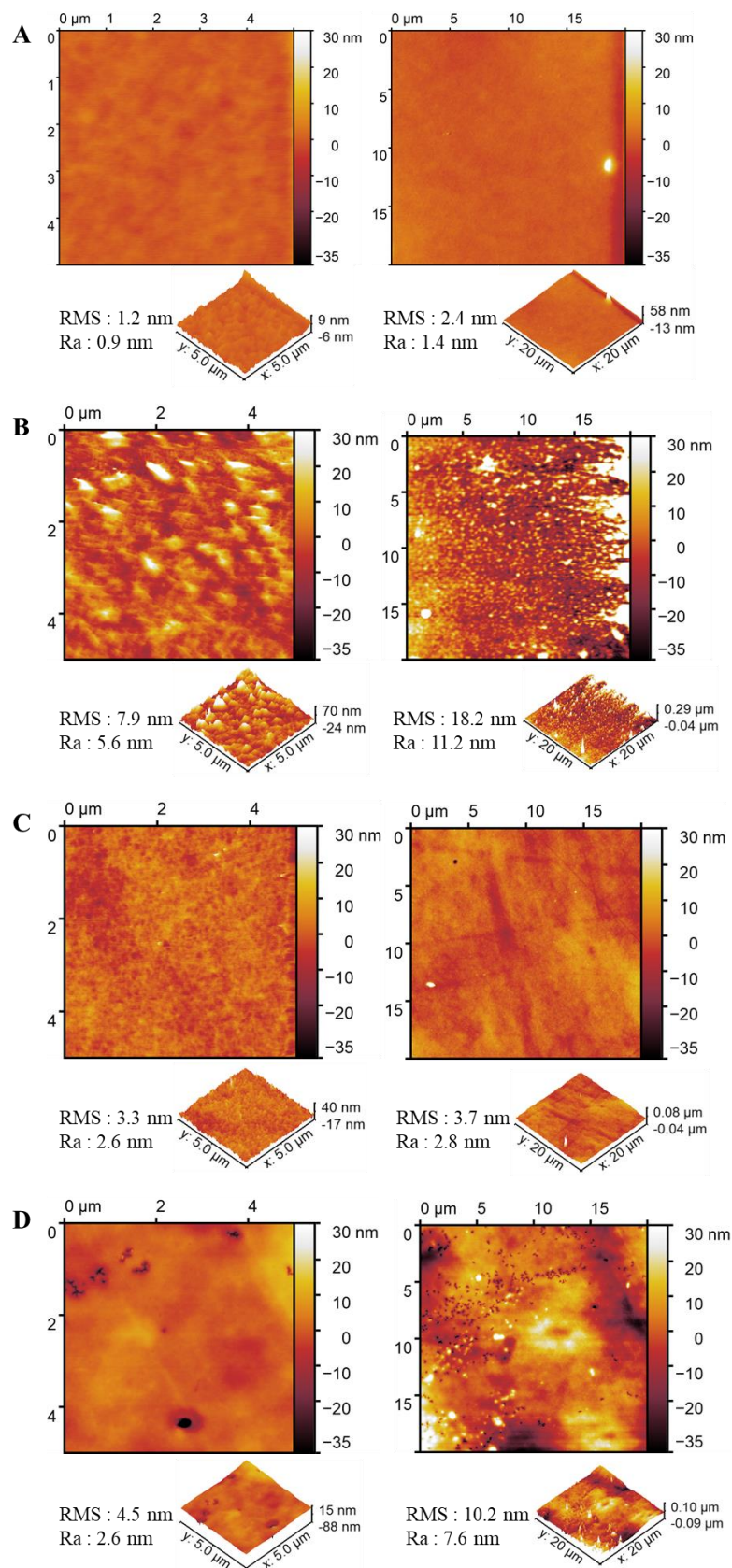


Figure 3. AFM images of (A) PDMS surface (control 1), (B) PDMS-PAONAI surface, (C) PDMS-T surface (control 4) and (D) PDMS-T-PAONAI surface.

The directly functionalized quaternary ammonium PDMS surface (PDMS-PAONAI) displayed an increased roughness around 11.2 nm with a lot of island suggesting an heterogenous grafting of the polymer (Figure 3-B). The roughness of the thiolated PDMS surface (PDMS-T) was around 2.8 nm without any aggregates (Figure 3-C), and increased to 7.6 nm after polymer grafting (PDMS-T-PAONAI) (Figure 3-D). However, a homogeneous grafting of the polymer was observed on the surface except for some areas where holes can be observed. AFM analysis confirmed contact angle and quaternary ammonium density values, i.e., that the thiolated cationic PDMS surface exhibited a higher surface coverage than the non thiolated one.

Spectroscopic surface characterizations

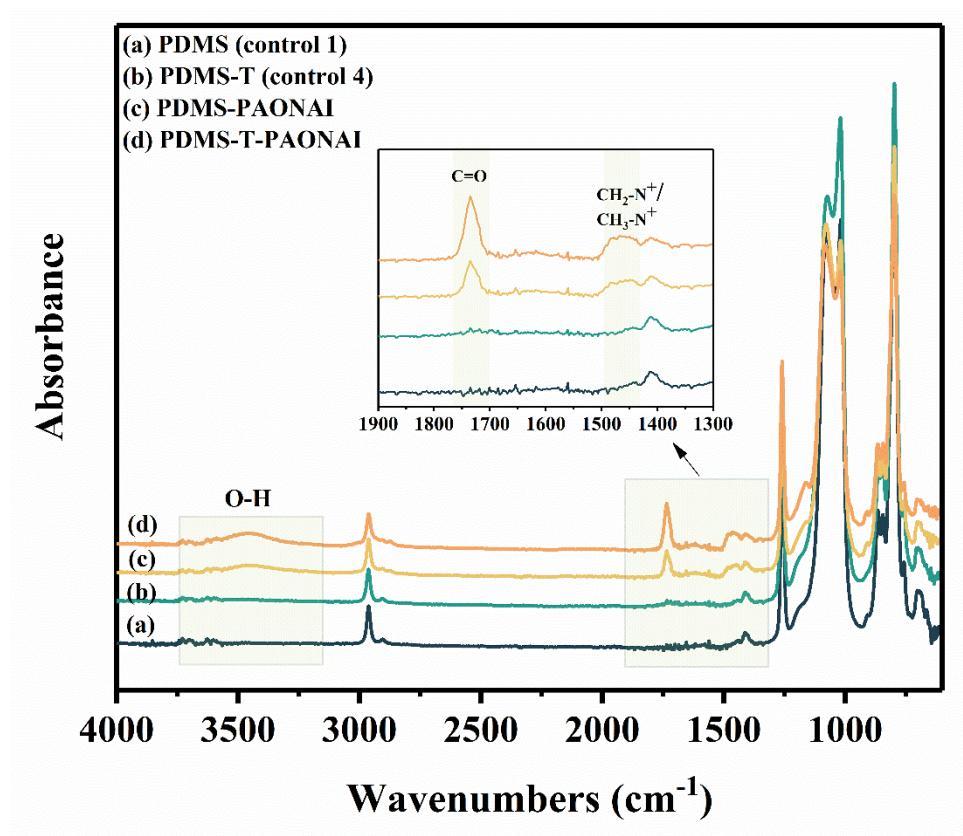


Figure 4. ATR-FTIR spectra of (a) PDMS (control 1), (b) PDMS-T (control 4), (c) PDMS-PAONAI and (d) PDMS-T-PAONAI.

The FTIR-ATR analysis (Figure 4 and the supporting information) of the prepared cationic surfaces, compared to their controls, showed the appearance of a new band at around 1730 cm⁻¹ arising from the carbonyl group of the grafted cationic polymer. The C-H bending vibration in N⁺-CH₂ and N⁺-CH₃ were observed between 1440 and 1498 cm⁻¹. A slight contribution of the butyl chain was also observed in the region of 2800 - 3100 cm⁻¹ (supplementary information). Due to the hygroscopic character of the cationic surface, one can

observe also a new band at 3300 cm⁻¹ arising from the moisture. The FTIR spectra of controls 1 to 5 were identical, suggesting that: 1- The grafted PTTMP formed a very thin monomolecular layer, which was not detected by this technique; 2- UV treatment was indispensable for the grafting reaction to occur; 3- the washing of the surface with methanol to remove the unreacted monomer was effective.

XPS analysis afforded the atomic compositions of the different modified and unmodified PDMS surfaces. The results are depicted in Table 3. As expected, XPS analysis of the PDMS reference surface shows the presence of carbon, oxygen and silicon (survey spectra in the supporting information). The atomic composition is close to the expected one for PDMS. A weak enrichment in silicon and oxygen, could be ascribed to residual SiO₂ coming from the synthesis process of the PDMS and also to residual Si-H groups after curing. After grafting, new characteristic elements of the grafted organic layers were observed by XPS. Thus, for the PDMS-PAONAI surface, nitrogen (1.4 at. %) and iodine (1.1 at. %) were detected in a close concentration, as expected. PDMS-T surface exhibited a sulfur composition of 1.7 at.%. For the PDMS-T-PAONAI surface, nitrogen (4.9 at. %), iodine (3.9 at. %) and sulfur (1 at. %) were observed. Combined to the increase of the C at. %, these results suggested a successful grafting for each step.

Actually, it is possible to determine an average thickness for each grafted layer. For the PDMS-PAONAI and PDMS-T, the thickness can be estimated using a simplified model considering a homogeneous and continuous organic layer on the top of the PDMS. For the PDMS-T-PAONAI which is composed of 2 distinct organic layers, a bilayer model has been used. Thus, the average thickness values have been calculated by solving the following set of three equations.

$$I_N = Kn_N^{PAONAI} \sigma_N \lambda_N^{PAONAI} T_N (1 - \exp(-\frac{d_{PAONAI}}{\lambda_N^{PAONAI}})) \quad (1)$$

$$I_S = Kn_S^T \sigma_S \lambda_S^T T_S (1 - \exp(-\frac{d_T}{\lambda_S^T})) \exp(-\frac{d_{PAONAI}}{\lambda_S^{PAONAI}}) \quad (2)$$

$$I_{Si} = Kn_{Si}^{PDMS} \sigma_{Si} \lambda_{Si}^{PDMS} T_{Si} \exp(-\frac{d_T}{\lambda_{Si}^T}) (\exp(-\frac{d_{PAONAI}}{\lambda_{Si}^{PAONAI}})) \quad (3)$$

With:

I: intensity of photoelectrons emitted by the element X; K: a spectrometer constant; σ : the photoionization cross section of the core level of the considered element; λ : the inelastic mean free path of the photoelectrons emitted by the core level of the considered element; n: the bulk

concentration; T: the transmission function for the electrons emitted by the core level of the element and d the thickness of the organic layer (values are given in the supplementary information).

The average thicknesses of the organic layer in PDMS-PAONAI and PDMS-T have been estimated to be 0.7 and 0.2 nm, respectively. For the PDMS-T-PAONAI, a similar average thickness (0.2 nm) was obtained for the intermediate Pentaerythritol tetrakis layer (T layer), whereas the PAONAI layer exhibited an average thickness of 2.6 nm. However, this method has some limitations: (i) The density of the grafted polymer is assimilated to the density of its monomer, i.e. around 1g/cm^3 , which is a rough approximation since the polymer is grafted as spaced brushes on the PDMS surface. The brushes could also contain ramifications due to chain transfer during the radical polymerization; (ii) The mathematical model doesn't take into account the surface roughness and the surface coverage by the grafted polymer. It considers that the polymer chains were perfectly arranged on the surface, which is also hypothetical and not actual; (iii) Since XPS detects only 10 nm of the extreme surface, the grafted density can be under estimated if the real thickness exceeds 10 nm, particularly in the case of the presence of islands. Usually, thicknesses obtained by this method are lower than 5 nm.

Thus, this method gives a way to express the polymer grafting density as an average thickness of a hypothetical homogeneous and compact polymer layer and not as an actual thickness. Indeed, if we take a look on AFM images, we can see that the difference in height between dark and light zones is around 60 nm. In addition, in many areas of the surface, the real thickness exceeded 10 nm, suggesting an under estimation of the grafting density and the average thicknesses determined by XPS.

Table 3. XPS elemental analysis of the optimal PDMS modified surface and its unmodified PDMS control

	C1s	O1s	Si2p	N1s	I3d	S2p
PDMS	43.4	26.4	30.2	--	--	--
PDMS-PAONAI	46.5	27.2	23.6	1.4	1.1	--
PDMS-T	47.1	28.3	22.9	--	--	1.7
PDMS-T-PAONAI	56.7	19.0	13.3	4.9	3.9	1.0

Assessment of the surface bactericidal properties

The bactericidal properties of the prepared cationic PDMS surfaces were studied by confocal fluorescent microscopy through the Live and Dead test, against *E. coli* (Gram-) and *S. epidermidis* (Gram+), two of the pathogens mostly involved in bacterial contaminations.

Actually, in the literature there are two suggested mechanisms for the bactericidal action of QA surfaces [38]. The most popular one suggests that long cationic polymer chains penetrate cells and thereby damage the membrane, like a needle that bursts a balloon. The second one suggests an ion exchange between the positive charges on the surface and the structurally critical mobile divalent cations within the membrane, which diffuse out of the membrane. The loss of these cations causes membrane destruction.

Bacteria were put in contact with the cationic surfaces as well as their controls during 1h, and then adhered bacteria were stained with a mixture of fluorescent probes that stained bacteria with damaged membrane in red and bacteria with intact membrane in green. The Live and Dead fluorescent images are presented in Figure 5 (and also in SI). One can observe that both thiolated (PDMS-T-PANONAI) and non-thiolated (PDMS-PANONAI) cationic PDMS surfaces exhibited a high bactericidal effect, i.e. quasi-only red bacteria were observed on contact with them (Figure 5-A2, B2, A4 and B4). Some residual green bacteria were observed in a few areas, often on other bacteria but not in contact with the cationic surface. Furthermore, the density of *E. coli* (Figure 5-A2 and A4) and *S. epidermidis* (Figure 5-B2 and B4) on the cationic surfaces was very high (around 10^6 cell/cm^2) and their attachment was very fast comparing to the non-cationic PDMS surfaces (controls 1 (PDMS) and 4 (PDMS-T)), for which no bacteria attachment was observed after 1h of contact. This suggests that the bacterial adhesion in this case is mainly governed by the electrostatic forces, since bacteria have an overall negative charge. This dependence of the bactericidal efficiency against *E. coli* and *S. epidermidis* as well as the bacterial adhesion on the charge density of cationic surfaces is in good agreement with the literature. For instance, the previously-mentioned azidated cationic PVC surface, grafted with an acrylate quaternary ammonium copolymer by the HDC click addition, exhibited a surface charge density around $6 \times 10^{14} \text{ charge.cm}^{-2}$, bacterial densities around $5 \times 10^5 \text{ cell/cm}^2$ with a killing efficiency around 99 % after 1h of contact [34]. Moreover, the prepared QA-PDMS surfaces displayed higher capacity in terms of bacterial killing capacity (around 100%) compared to analogues prepared by the hydrosilylation process after full PDMS curing (around 96%) [13]. On the other hand, the analogue surfaces prepared before curing or

with higher Si-H content in the component mixture led to similar short-term bactericidal effect [13].

Moreover, the long-term biocidal functionality of QA coatings depends on the surface charge density and also on the concentration of the bacteria exposed to the surface (the challenge). Murata *et al.* [38] have shown that cationic surfaces with charge densities above $5 \cdot 10^{15}$ charges/cm², are able to kill at least a monolayer of *E. coli* cells (10^8 CFU/cm²), before going through fouling and loss of bioactivity. Under real-world conditions, extreme infection or contamination occurs when the bacterial concentration is about 10^3 CFU/cm², which is far from the concentration that passivates the prepared cationic surface with around 10^{17} charges/cm². Therefore, the passivating bacterial concentration, can take a very long time to be reached, depending on the number of bacteria to which this surface is exposed.

Finally, quaternary ammonium may exhibit cytotoxicity in solution, depending on concentration, time exposure and chemical structure [39-41]. However, the biocompatibility of QA surfaces needs further investigations to define clearly their potential of application in the medical field [42]. Elsewhere [13], we have established that plasmatic proteins, owing to their electrical charges, adsorbed on QA surfaces, which caused their fouling after only 24 hours of contact. Therefore, at this time, we can suggest to employ this kind of surface in non-blood contact silicone devices, such as the external surfaces of catheter chambers and extracorporeal equipment.

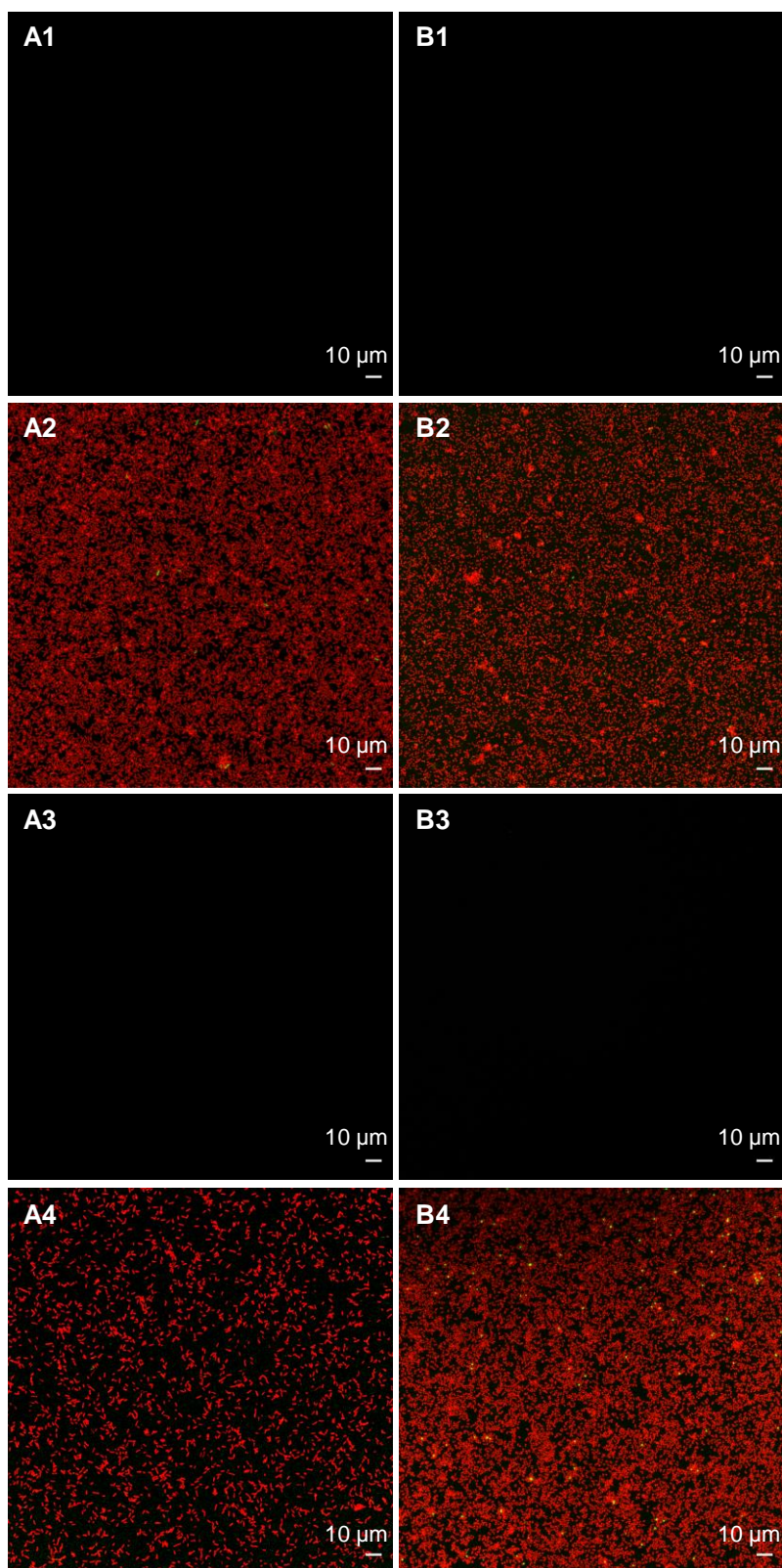


Figure 5. Fluorescence microscopy images of sessile bacteria cells stained with a marker of viability and deposited on surfaces of modified and unmodified PDMS surfaces: (A1) *E. coli* on unmodified PDMS surface (control 1), (A2) *E. coli* on cationic PDMS-PAONAI surface, (A3) *E. coli* on PDMS-T surface (control 5), (A4) *E. coli* on cationic PDMS-T-PANONAI surface, (B1) *S. epidermidis* on unmodified PDMS surface (control 1), (B2) *S. epidermidis* on cationic PDMS-PAONAI surface, (B3) *S. epidermidis* on PDMS-T surface (control 5), (B4) *S. epidermidis* on cationic PDMS-T-PANONAI surface.

Conclusion

In this work, we have evidenced the possibility of designing bactericidal cationic PDMS surfaces, with tunable quaternary ammonium content and hydrophilicity, by a benzophenone photo-induced polymerization of an acrylate ammonium monomer from native and thiolated PDMS surfaces. The direct photopolymerization led to an optimal PDMS surface with a water contact angle around 75° and a charge density around $10^{15} \text{ N}^+.\text{cm}^{-2}$, i.e. like a ‘grafting to’ method. Pretreatment of the PDMS surface by thiolation led to cationic PDMS surfaces with increased surface hydrophilicity (contact angle around 28°) and increased charge density to around $10^{17} \text{ N}^+.\text{cm}^{-2}$. The Live and Dead test by fluorescence microscopy revealed an efficient contact killing of all the prepared cationic surfaces against *E. coli* and *S. epidermidis*. By increasing the surface charge density, the longevity of the cationic PDMS surface was implicitly enhanced. The prepared surfaces can be intended for application as biomaterials or medical devices without contact with blood.

Acknowledgments

Authors thanks the INSA ROUEN NORMANDIE and the China Scholarship Council (CSC) for the financial supports.

Data availability statement

The raw/processed data required to reproduce these findings cannot be shared at this time due to technical or time limitations.

References

- [1] A. B. Swanson, "Silicone Rubber Implants for Replacement of Arthritic or Destroyed Joints in the Hand," *Surg. Clin. North Am.*, vol. 48, no. 5, pp. 1113–1127, 1968.
- [2] M. Bračič, O. Sauperl, S. Strnad, I. Kosalec, O. Plohl, L. F. Zemljič. "Surface modification of silicone with colloidal polysaccharides formulations for the development of antimicrobial urethral catheters," *Appl. Surf. Sci.*, vol. 463, no. 1, pp. 889-899, 2019.
- [3] A. Colas and J. Curtis, "Silicone biomaterials: history and chemistry," *Biomater. Sci. an Introd. to Mater. Med.*, vol. 2, pp. 80–85, 2004.
- [4] A. U. Daniels, "Silicone breast implant materials," *Swiss Med. Wkly.*, vol. 142, no. JULY, 2012.
- [5] K. W. Dunn, P. N. Hall, and C. T. K. Khoo, "Breast implant materials: sense and safety," *Br. J. Plast. Surg.*, vol. 45, no. 4, pp. 315–321, 1992.
- [6] A. Colas, "Silicones: preparation, properties and performance," *Dow Corning, Life Sci.*, 2005.
- [7] J. R. Henstock, L. T. Canham, and S. I. Anderson, "Silicon: the evolution of its use in biomaterials," *Acta Biomater.*, vol. 11, pp. 17–26, 2015.
- [8] A. I. Doulgeraki, P. Di Ciccio, A. Ianieri, and G. J. E. Nychas, "Methicillin-resistant food-related *Staphylococcus aureus*: a review of current knowledge and biofilm formation for future studies and applications," *Res. Microbiol.*, vol. 168, no. 1, pp. 1–15, 2017.
- [9] A. Tripathy, A. Kumar, S. Sreedharan, G. Muralidharan, A. Pramanik, D. Nandi, and P. Sen, "Fabrication of Low-Cost Flexible Superhydrophobic Antibacterial Surface with Dual-Scale Roughness," *ACS Biomaterials Science and Engineering*, vol. 4, no. 6, pp. 2213-2223, 2018.
- [10] A. Tripathy, A. Kumar, A. R. Chowdhury, K. Karmakar, S. Purighalla, V. K. Sambandamurthy, D. Chakravorty and P. Sen, "A Nanowire-Based Flexible Antibacterial Surface Reduces the Viability of Drug-Resistant Nosocomial Pathogens," *ACS Applied Nano Materials*, vol. 1, no. 6, pp. 2678-2688, 2018.
- [11] C. Donzel *et al.*, "Hydrophilic poly (dimethylsiloxane) stamps for microcontact printing," *Adv. Mater.*, vol. 13, no. 15, pp. 1164–1167, 2001.
- [12] A. Oláh, H. Hillborg, and G. J. Vancso, "Hydrophobic recovery of UV/ozone treated poly (dimethylsiloxane): adhesion studies by contact mechanics and mechanism of surface modification" *Appl. Surf. Sci.*, vol. 239, no. 3–4, pp. 410–423, 2005.
- [13] N. Kébir, I. Kriegel, M. Estève, and V. Semetey, "Preparation of bactericidal cationic PDMS surfaces using a facile and efficient approach," *Appl. Surf. Sci.*, vol. 360, pp. 866–874, 2016.
- [14] W. Mussard, N. Kebir, I. Kriegel, M. Estève, and V. Semetey, "Facile and efficient control of bioadhesion on poly(dimethylsiloxane) by using a biomimetic approach," *Angew. Chemie*, vol. 123, no. 46, pp. 11063–11066, 2011.
- [15] D.-J. Guo, H.-M. Han, S.-J. Xiao, and Z.-D. Dai, "Surface-hydrophilic and protein-resistant silicone elastomers prepared by hydrosilylation of vinyl poly(ethylene glycol) on hydrosilanes-poly (dimethylsiloxane) surfaces," *Colloids Surfaces A Physicochem. Eng. Asp.*, vol. 308, no. 1–3, pp. 129–135, 2007.
- [16] Y. Wu, Y. Huang, and H. Ma, "A facile method for permanent and functional surface modification of poly(dimethylsiloxane)," *J. Am. Chem. Soc.*, vol. 129, no. 23, pp. 7226–7227, 2007.
- [17] H. Chen, Y. Chen, H. Sheardown, and M. A. Brook, "Immobilization of heparin on a silicone surface through a heterobifunctional PEG spacer," *Biomaterials*, vol. 26, no. 35, pp. 7418–7424, 2005.

- [18] H. Chen, Z. Zhang, Y. Chen, M. A. Brook, and H. Sheardown, "Protein repellent silicone surfaces by covalent immobilization of poly(ethylene oxide)," *Biomaterials*, vol. 26, no. 15, pp. 2391–2399, 2005.
- [19] Y. Wang, H.-H. Lai, M. Bachman, C. E. Sims, G. P. Li, and N. L. Allbritton, "Covalent micropatterning of poly(dimethylsiloxane) by photografting through a mask," *Anal. Chem.*, vol. 77, no. 23, pp. 7539–7546, 2005.
- [20] S. Sugiura, J. Eda Hiro, K. Sumaru, and T. Kanamori, "Surface modification of polydimethylsiloxane with photo-grafted poly (ethylene glycol) for micropatterned protein adsorption and cell adhesion," *Colloids Surfaces B Biointerfaces*, vol. 63, no. 2, pp. 301–305, 2008.
- [21] B. L. Leigh, E. Cheng, L. Xu, A. Derk, M. R. Hansen, and C. A. Guymon, "Antifouling photograftable zwitterionic coatings on PDMS substrates," *Langmuir*, vol. 35, no. 5, pp. 1100–1110, 2018.
- [22] A. I. Khalaf, Y. Assem, A. A. Yehia, A. M. Rabia, and T. A. Zidan, "Optical, dielectric, and mechanical properties of exfoliated poly (N, N- dimethylaminoethyl methacrylate)/Clay nanocomposites prepared via In- situ bulk polymerization," *Polym. Compos.*, vol. 39, no. 8, pp. 2603–2610, 2018.
- [23] C. Zhou, M. D. Weir, K. Zhang, D. Deng, L. Cheng, and H. H. K. Xu, "Synthesis of new antibacterial quaternary ammonium monomer for incorporation into CaP nanocomposite," *Dent. Mater.*, vol. 29, no. 8, pp. 859–870, 2013.
- [24] D. C. Grothe, W. Meyer, and S. Janietz, "Acrylate functionalized tetraalkylammonium salts with ionic liquid properties," *Molecules*, vol. 17, no. 6, pp. 6593–6604, 2012.
- [25] Schneider, C.A., Rasband, W.S., Eliceiri, K.W. "NIH Image to ImageJ: 25 years of image analysis," *Nature Methods* vol. 9, no. 7 pp. 671-675, 2012.
- [26] W. Zhong, C. Dong, R. Liuyang, Q. Guo, H. Zeng, Y. Lin, A. Zhang, "Controllable synthesis and antimicrobial activities of acrylate polymers containing quaternary ammonium salts," *React. Funct. Polym.*, vol. 121, pp. 110-118, 2017.
- [27] J. G. Lundin, P. N. Coneski, P. A. Fulmer, J. H. Wynne, "Relationship between surface concentration of amphiphilic quaternary ammonium biocides in electrospun polymer fibers and biocidal activity," *React. Funct. Polym.*, vol. 77, pp. 39-46, 2014.
- [28] Z. Huang, R. Liuyang, C. Dong, Y. Lei, A. Zhang, Y. Lin, "Polymeric quaternary ammonium salt activity against *Fusarium oxysporum* f. sp. *cubense* race 4: Synthesis, structure-activity relationship and mode of action," *React. Funct. Polym.*, vol. 114, pp. 13-22, 2017.
- [29] A. Palantoken, M. S. Yilmaz, N. A. Unubol, E. Yenigul, S. Pişkin, T. Eren, "Synthesis and characterization of a ROMP-based polycationic antimicrobial hydrogel," *Eur. Polym. J.*, vol. 112, pp. 365-375, 2019.
- [30] B. Dizman, M. O. Elasri, and L. J. Mathias, "Synthesis and antimicrobial activities of new water- soluble bis- quaternary ammonium methacrylate polymers," *J. Appl. Polym. Sci.*, vol. 94, no. 2, pp. 635–642, 2004.
- [31] D. Sha, J. Xu, X. Yang, Y. Xue, X. Liu, C. Li, M. Wei, Z. Liang, K. Shi, B. Wang, Y. Tang, X. Ji, "Synthesis and antibacterial activities of quaternary ammonium salts with different alkyl chain lengths grafted on polyvinyl alcohol-formaldehyde sponges," *React. Funct. Polym.*, vol. 158, pp. 104797, 2021.
- [32] J. Guo et al., "Antibacterial activity of cationic polymers: side-chain or main-chain type?," *Polym. Chem.*, vol. 9, no. 37, pp. 4611–4616, 2018.

- [33] G. Lu, D. Wu, R. Fu, "Studies on the synthesis and antibacterial activities of polymeric quaternary ammonium salts from dimethylaminoethyl methacrylate," *React. Funct. Polym.*, vol. 67, no. 4, pp. 355-366, 2007.
- [34] J. Lafarge, N. Kebir, D. Schapman, and F. Burel, "Design of self-disinfecting PVC surfaces using the click chemistry," *React. Funct. Polym.*, vol. 73, no. 11, pp. 1464–1472, 2013.
- [35] Y. Jiao, L. Niu, S. Ma, J. Li, F. R. Tay, and J. Chen, "Quaternary ammonium-based biomedical materials: State-of-the-art, toxicological aspects and antimicrobial resistance," *Prog. Polym. Sci.*, vol. 71, pp. 53–90, 2017.
- [36] T. Zhou et al., "Surface functionalization of biomaterials by radical polymerization," *Prog. Mater. Sci.*, vol. 83, pp. 191–235, 2016.
- [37] J. C. Tiller, C.-J. Liao, K. Lewis, and A. M. Klibanov, "Designing surfaces that kill bacteria on contact," *Proc. Natl. Acad. Sci.*, vol. 98, no. 11, pp. 5981–5985, 2001.
- [38] H. Murata, R. R. Koepsel, K. Matyjaszewski, and A. J. Russell, "Permanent, non-leaching antibacterial surfaces-2: How high density cationic surfaces kill bacterial cells," *Biomaterials*, vol. 28, no. 32, pp. 4870–4879, 2007.
- [39] C. Debbasch, M.D. St Jean, P.J. Pisella, P. Rat, J.M. Warnet, C. Baudouin. "Quaternary ammonium cytotoxicity in a human conjunctival cell line," *J Fr Ophtalmol.*, vol. 22, no. 9, pp. 950-958, 1999.
- [40] D. Fischer, Y. Li, B. Ahlemeyer, J. Krieglstein, T. Kissel, "In vitro cytotoxicity testing of polycations: influence of polymer structure on cell viability and hemolysis," *Biomaterials*, vol. 24, no. 7, pp. 1121-1131, 2003.
- [41] T. Eren, A. Som, J. R. Rennie, C. F. Nelson, Y. Urgina, K. Nüsslein, E. B. Coughlin, G. N. "Tew. Antibacterial and Hemolytic Activities of Quaternary Pyridinium Functionalized Polynorbornenes," *Macromol. Chem. Phys.*, vol. 209, pp. 516–524, 2008.
- [42] H. Bouloussa, A.Saleh- mghir, C. Valotteau, C. Cherifi, N. Hafsia, et al.. "A Graftable Quaternary Ammonium Biocidal Polymer Reduces Biofilm Formation and Ensures Biocompatibility of Medical Devices," *Advanced Materials Interfaces*, vol. 8, no. 5, pp.2001516, 2021.

Declaration of interests

☒ The authors declare that they have no known competing financial interests or personal relationships that could have appeared to influence the work reported in this paper.

☐The authors declare the following financial interests/personal relationships which may be considered as potential competing interests:

Yuzhen LOU: Investigation, formal analysis, Data Curation, writing.

Damien SCHAPMAN: formal analysis, Data Curation

Dimitri MERCIER: formal analysis, Data Curation

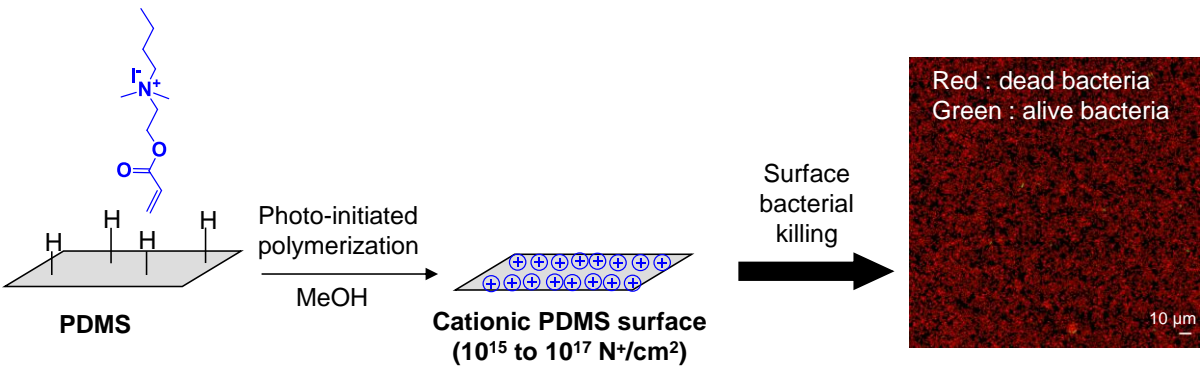
Stéphane ALEXANDRE: formal analysis, Data Curation

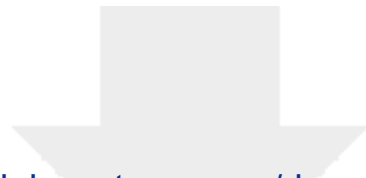
Fabrice BUREL: Project administration.

Pascal THEBAULT: methodology, Validation, supervision, writing.

Nasreddine KEBIR: Funding acquisition, project administration, conceptualization, methodology, validation, supervision, writing.

- Preparation of highly quaternary ammonium functionalized PDMS surfaces by two 'grafting from' processes.
- Photo-initiated polymerization of *N*-[2-(acryloyloxy)ethyl]-*N,N*-dimethyl-*N*-butylammonium iodide from native and thiolated PDMS surfaces.
- The direct grafting led to surface charge densities around 10^{15} charge/cm².
- The indirect grafting led to surface charge densities around 10^{17} charge/cm².
- The obtained surfaces effectively kill surface bacteria.





[Click here to access/download](#)

Supplementary Material

Revised Supporting information.docx

